

Spectrum of Controlling and Observing Complex Networks

Gang Yan^{1†}, Georgios Tsekenis^{1†}, Baruch Barzel², Jean-Jacques Slotine³, Yang-Yu Liu^{4,5}, Albert-László Barabási^{1,4,5,6*}

¹*Center for Complex Network Research and Department of Physics, Northeastern University, Boston, Massachusetts 02115, USA*

²*Department of Mathematics, Bar-Ilan University, Ramat-Gan 52900, Israel*

³*Department of Mechanical Engineering and Department of Brain and Cognitive Sciences, Massachusetts Institute of Technology, Cambridge, Massachusetts 02139, USA*

⁴*Department of Medicine and Division of Network Medicine, Brigham and Women's Hospital, Harvard Medical School, Boston, Massachusetts 02115, USA*

⁵*Center for Cancer Systems Biology, Dana Farber Cancer Institute, Boston, Massachusetts 02115, USA*

⁶*Center for Network Science, Central European University, H-1051 Budapest, Hungary*

[†]These authors contributed equally to this work.

*Corresponding author. Email: alb@neu.edu

Observing and controlling complex networks are of paramount interest for understanding complex physical, biological and technological systems. Recent studies have made important advances in identifying sensor or driver nodes, through which we can observe or control a complex system. Yet, the observation uncertainty induced by measurement noise and the energy cost required for control continue to be significant challenges in practical applications. Here we show that the control energy cost and the observation uncertainty vary widely in different directions of the state space. In particular, we find that if all nodes are directly driven, control is energetically feasible, as the maximum energy cost increases sublinearly with the system size. If, however, we aim to control a system by driving only a single node, control in some directions is energetically prohibitive, increasing exponentially with the system size. For the cases in between, the maximum energy decays exponentially if we increase the number of driver nodes. We validate our findings in both model systems and real networks. Our results provide fundamental laws that deepen our understanding of diverse complex systems.

Introduction

Many natural and man-made systems can be represented as networks¹⁻³, where nodes are the system's components and links describe the interactions between them. Thanks to these interactions, perturbations of one node can alter the states of the other nodes. This property has been exploited to control a network, i.e., to move it from an initial state to a desired final state⁴⁻⁶ by manipulating the state variables of only a subset of its nodes⁷. Such control processes⁷⁻¹⁹ play an important role in the regulation of protein expression²⁰, the coordination of moving robots²¹, and the inhibition

of undesirable social contagions²². At the same time the interdependence between nodes means that the states of a small number of sensor nodes contain sufficient information about the rest of the network, so that we can reconstruct the system's full internal state by accessing only a few outputs²³. This can be utilized for biomarker design in cellular networks, or to monitor in real time the functionality of infrastructural²⁴ and social-ecological²⁵ systems for early warning of failures or disasters²⁶.

While recent advances in driver and sensor node identification constitute unavoidable steps towards controlling and observing real networks, in practice we continue to face significant challenges: the control of a large network may require a vast amount of energy¹²⁻¹⁴ and measurement noise²⁷ causes uncertainties in the observation process. To quantify these issues we formalize the dynamics of a controlled network with N nodes and N_D external control inputs as⁴⁻⁷

$$\dot{\mathbf{x}}(t) = A\mathbf{x}(t) + B\mathbf{u}(t), \quad (1)$$

where the vector $\mathbf{x}(t) = [x_1(t), x_2(t), \dots, x_N(t)]^T$ describes the states of the N nodes at time t . In (1) $x_i(t)$ can represent the concentration of a metabolite in a metabolic network²⁸, the geometric state of a chromosome in a chromosomal interaction network¹⁰, or the belief of an individual in opinion dynamics^{22,29}. The vector $\mathbf{u}(t) = [u_1(t), u_2(t), \dots, u_{N_D}(t)]^T$ represents the external control inputs, and B is the input matrix with $B_{ij} = 1$ if the control input $u_j(t)$ is imposed on node i . The adjacency matrix A captures the interactions between the nodes, including the possibility of self-loops A_{ii} representing the self-regulation of node i .

The system (1) can be driven from an initial state \mathbf{x}_o to any desired final state \mathbf{x}_d within

the time $t \in [0, \tau]$ using an infinite number of possible control inputs $\mathbf{u}(t)$. The optimal input vector aims to minimize the energy cost⁴ $\int_0^\tau \|\mathbf{u}(t)\|^2 dt$, which captures the energy of electronic and mechanic systems or the amount of effort required to control biological and social systems. If at $t = 0$ the system is in state $\mathbf{x}_o = \mathbf{0}$, the minimum energy required to move the system to point \mathbf{x}_d in the state space is^{4,12,13}

$$\mathcal{E}(\tau) = \mathbf{x}_d^T G_c^{-1}(\tau) \mathbf{x}_d, \quad (2)$$

where $G_c(\tau) = \int_0^\tau e^{At} B B^T e^{A^T t} dt$ is the symmetric controllability Gramian. When the system is controllable all eigenvalues of $G_c(\tau)$ are positive. Eq. (2) indicates that for a network A and an input matrix B the control energy $\mathcal{E}(\tau)$ also depends on the desired state \mathbf{x}_d . Consequently, driving a network to various directions in the state space requires different amounts of energy. For example, to move the weighted network of Fig. 1a to the three different final states \mathbf{x}_d with $\|\mathbf{x}_d\| = 1$, we inject the optimal signals $\mathbf{u}(t)$ shown in Fig. 1b onto node 1, steering the system along the trajectories shown in Fig. 1c. The corresponding minimum energies are shown in Fig. 1d. The control energy surface for all normalized desired states is an ellipsoid, implying that the required energy varies dramatically as we move the system in different directions.

Results

As real systems normally function near a stable state, i.e., all eigenvalues of A are negative³⁰, the control energy $\mathcal{E}(\tau)$ decays quickly to a nonzero stationary value when the control time τ increases¹². Henceforth we focus on the control energy $\mathcal{E} \equiv \mathcal{E}(\tau \rightarrow \infty)$ and the controllability Gramian $G \equiv G_c(\tau \rightarrow \infty)$.

Given a network A and an input matrix B , the controllability Gramian G is unique, embodying all properties related to the control of the system. To uncover the direction of the state space requiring different energies, we explore the eigen-space of G . Denote by \mathcal{E}_i the eigen-energies, i.e., the minimum energy required to drive the network to G 's eigen-directions. According to Eq. (2) $\mathcal{E}_i = 1/\mu_i$ with μ_i corresponding to G 's eigenvalues. Generally, the energy surface for a network with N nodes is a super-ellipsoid spanned by G 's N eigen-directions. To determine the distribution of these eigen-energies we decompose the adjacency matrix as $A = V\Lambda V^T$, where V represents the eigenvectors of A and $\Lambda = \text{diag}\{-\lambda_1, -\lambda_2, \dots, -\lambda_N\}$ are the eigenvalues. (For stable undirected networks all eigenvalues of A are negative, thus we denote the eigenvalues by $-\lambda_i$ so that the absolute eigenvalues are $\lambda_i > 0$ for all i .) We sort the absolute eigenvalues in ascending order $0 < \lambda_1 < \lambda_2 < \dots < \lambda_N$, and find that (SI Sec. I)

$$G = V[(V^T B B^T V) \circ C]V^T, \quad (3)$$

where \circ denotes Hadamard product, i.e., $(X \circ Y)_{ij} = X_{ij}Y_{ij}$, and C is a matrix with entries $C_{ij} = \frac{1}{\lambda_i + \lambda_j}$. For a given network, (3) captures the impact of the input matrix B on the control properties of the system, allowing us to analyze the distribution of eigen-energies for different number of driver nodes and determine the required energy for each direction.

Controlling all nodes

If we can control all nodes, i.e., $N_D = N$, B becomes a unit diagonal matrix. In this case $G = V\text{diag}\{\frac{1}{2\lambda_i}\}V^T$ and the eigen-directions of the controlled system are the same as the network's eigenvectors. Thus $\mathcal{E}_i = 2\lambda_i$ and $p(\mathcal{E}) = p(\lambda)$, i.e., the distribution of eigen-energies is identical to the distribution of the network's absolute eigenvalues. We add self-loops as $A_{ii} = -(\delta + \sum_{j=1}^N A_{ij})$

where $\delta > 0$ is a small perturbation to ensure that all eigenvalues of A are negative. This scheme has been widely used in previous studies on dynamical processes taking place on networks, such as opinion dynamics²², synchronization³¹, and control¹². For networks with degree distribution¹⁻³ $p(k) \sim k^{-\gamma}$ the distribution of A 's absolute eigenvalues also obeys a power law^{32,33} $p(\lambda) \sim \lambda^{-\gamma}$ (see SI Sec. II A). Consequently,

$$p(\mathcal{E}) \sim \mathcal{E}^{-\gamma}, \quad (4)$$

indicating that most directions of the state space are easily controlled, requiring a small \mathcal{E} . A few directions require considerable energy. The most difficult direction needs³⁴ $\mathcal{E}_{\max} \sim N^{\frac{1}{\gamma-1}}$. The fact that \mathcal{E}_{\max} is sub-linear in N for $\gamma > 2$ indicates that the required energy remains bounded, hence there are no significant energetic barriers for control with $N_D = N$. As shown in Fig. 2b, for the scale-free model³⁵ and the *S. cerevisiae* protein-protein interaction³⁶ networks $p(\mathcal{E})$ indeed follows a power law; in contrast for the Erdős-Rényi random network³⁷ and the US power grid³⁸ $p(\mathcal{E})$ are bounded (Fig. 2a), as predicted by $\gamma \rightarrow \infty$ in (4), requiring even less energy for control.

Controlling a single node

If each node has a nonidentical self-loop we can control an undirected network by driving only a single node³⁹. In this case $V^T B B^T V = \{V_{ih} V_{jh}\} \sim \mathcal{O}(1/N)$, where h is the index of the single driver node. Thus $V^T B B^T V$ can be viewed as a small perturbation to the matrix C in (3). The statistical behavior of G 's eigenvalues is mainly determined by the eigenvalues of C , whose distribution can be approximated as $p(\mathcal{E}) \sim 1/(1 + 1/\mathcal{E})\mathcal{E}^{-1}$ (see SI Sec. IIIA, B for details). Therefore,

$$p(\mathcal{E}) \sim \mathcal{E}^{-1} \quad (5)$$

for large \mathcal{E} . Eq. (5) predicts that, to drive a network of N nodes with a single driver node, the most difficult direction in the state space requires $\mathcal{E}_{\max} \sim e^N$ energy (SI Sec. III C). This exponential N -dependence makes the control of large networks (N) in the most difficult direction energetically infeasible. For validation we also consider the complementary cumulative distribution $p_{>}(\mathcal{E}) = \int_{\mathcal{E}}^{\mathcal{E}_{\max}} p(\mathcal{E}') d\mathcal{E}'$. Based on (5) we obtain $p_{>}(\mathcal{E}) \sim (\ln \mathcal{E}_{\max} - \ln \mathcal{E})$, decreasing linearly with $\ln \mathcal{E}$. This is confirmed for both Erdős-Rényi and scale-free network models in Fig 2(c). For the numerical feasibility we also test the distribution on two moderate-size empirical networks: a terrorist communication network⁴⁰ where A_{ij} represents the interaction frequency between i and j ; and a mutualistic ecological network⁴¹ where weighted edges describe interaction strength between species. As shown in Fig 2(d), although there are deviations due to degree correlations⁴², the presence of communities⁴³ and nestedness⁴⁴ characterizing these networks, the corresponding eigen-energies span over a hundred of orders of magnitude and are reasonably well approximated by (5).

Controlling a finite fraction of nodes

When $p(\mathcal{E}) \sim \mathcal{E}^{-\gamma}$, the distribution $p(\hat{\mathcal{E}}) \sim e^{(1-\gamma)\hat{\mathcal{E}}}$ where $\hat{\mathcal{E}} \equiv \ln \mathcal{E}$. Thus, if $N_D = N$, $p(\hat{\mathcal{E}})$ is an exponential (one-peak) distribution as $\gamma > 2$ in (4); if $N_D = 1$, as $p(\mathcal{E}) \sim \mathcal{E}^{-1}$ in (5), $p(\hat{\mathcal{E}})$ is a uniform distribution. To understand the transition from (4) for $N_D = N$ to (5) for $N_D = 1$, we investigate the distribution $p(\hat{\mathcal{E}})$ when $1 < N_D < N$, i.e., controlling a finite fraction of nodes. In this case, we find that $p(\hat{\mathcal{E}})$ has multiple peaks (Fig. 3a), which is induced by the gaps in the eigen-energy spectrum (Fig. 3b). For $N_D/N = 0.6$, there is a gap separating the eigen-energies into two bands and the lower band contains N_D eigen-energies. This gap leads to two peaks in the

distribution $p(\hat{\mathcal{E}})$ as shown in Fig. 3c. When we have fewer driver nodes (N_D/N decreases), the number of peaks N_{peak} increases (Fig. 3a). We find that $N_{\text{peak}} = \text{int}[N/N_D]$, i.e., $N_{\text{peak}} = 2, 4, 5$ for $N_D/N = 0.5, 0.25, 0.2$ respectively (see also SI Fig. S3). The multi-peak nature of $p(\hat{\mathcal{E}})$ has two important implications. First, the boundary of the first energy band \mathcal{E}_{N_D} varies only weakly with N_D (Fig. 3d), indicating that the energy required to move the network within the subspace spanned by the first N_D eigen-directions is relatively small. Second, $\hat{\mathcal{E}}$ (i.e., $\log \mathcal{E}$) grows linearly from one band to the next (SI Fig. S4). Thus, $\log \mathcal{E}_{\text{max}}$ (the boundary of the last band) is linearly dependent of the number of peaks, i.e., $\mathcal{E}_{\text{max}} \sim e^{N/N_D}$ (Fig. 3d). Consequently, controlling a single node induces N peaks in $p(\hat{\mathcal{E}})$, i.e., the distribution $p(\hat{\mathcal{E}})$ becomes uniform (SI Fig. S3), resulting in $p(\mathcal{E}) \sim \mathcal{E}^{-1}$ of (5) and $\mathcal{E}_{\text{max}} \sim e^N$. We summarize our findings about the largest energy and the distribution of eigen-energies in Table 1.

Implications to observation uncertainty

The results obtained above have direct implications for observability as well. Indeed, consider the dynamics

$$\dot{\mathbf{x}}(t) = A\mathbf{x}(t) \tag{6}$$

$$\mathbf{y}(t) = C\mathbf{x}(t) + \mathbf{w}(t) \tag{7}$$

with an initial state $\mathbf{x}_o \neq 0$, where C is the output matrix and $\mathbf{y}(t)$ are the output signals including measurement noise $\mathbf{w}(t)$, which we assume to be a Gaussian white noise with zero mean and variance one. We aim to estimate $\hat{\mathbf{x}}_o$ of the initial state \mathbf{x}_o while minimizing the difference $\int_0^\tau \|\mathbf{y}(t) - \hat{\mathbf{y}}(t)\|^2 dt$ between the output $\mathbf{y}(t)$ that is actually observed and the output $\hat{\mathbf{y}}(t) = Ce^{At}\hat{\mathbf{x}}_o$

that would be observed in the absence of noise. With the maximum-likelihood approximation⁴⁵, the expectation $\langle \hat{\mathbf{x}}_o \rangle = \mathbf{x}_o$ and the covariance matrix⁴⁵ $\langle \tilde{\mathbf{x}}\tilde{\mathbf{x}}^T \rangle = G_o^{-1}(\tau)$, where $\tilde{\mathbf{x}} \equiv \hat{\mathbf{x}}_o - \mathbf{x}_o$ is estimation error and $G_o(\tau) = \int_0^\tau e^{A^T t} C^T C e^{A t} dt$ is the observability Gramian. Therefore, the variance σ^2 of the approximation in direction $\tilde{\mathbf{x}}$ is

$$\sigma^2(\tau) = \tilde{\mathbf{x}}^T G_o^{-1}(\tau) \tilde{\mathbf{x}}, \quad (8)$$

indicating that the estimation uncertainty varies with the direction of the state space. For instance, when the network in Fig. 1e moves along the trajectory of Fig. 1g, we measure the state of the sensor node and plot the noisy output $\mathbf{y}(t)$ in Fig. 1f. With the maximum-likelihood approximation we reconstruct \mathbf{x}_o from $\mathbf{y}(t)$ and show the estimation error $\tilde{\mathbf{x}} \equiv \hat{\mathbf{x}}_o - \mathbf{x}_o$ for thousands of independent runs (Fig. 1h). The estimation variance is different for various directions, forming an uncertainty ellipsoid. Thanks to the duality between $G_c(\tau)$ and $G_o(\tau)$, the control energy for a direction in Fig. 1d represents the estimation variance for the same direction in Fig. 1h.

To be specific, for the controllability Gramian G_c in (2) and the observability Gramian G_o in (5), we have $\sigma^2 = \mathcal{E}$ for the same direction, i.e., the less controllable directions (requiring larger energy) are also less observable (having higher uncertainty). Therefore, our findings about the distribution of eigen-energies apply directly to the distribution of σ^2 along the eigen-directions: if the number of sensor nodes $N_S = N$, we have $p(\sigma^2) \sim (\sigma^2)^{-\gamma}$; if $N_S = 1$, we have $p(\sigma^2) \sim (\sigma^2)^{-1}$; and if $1 < N_S < N$, there are N/N_S peaks in the distribution of $p[\log \sigma^2]$. The high heterogeneity of observation uncertainty indicates that, if we monitor only a small fraction of nodes, most directions of the state space are easily observable but the observation can be extremely unreliable for a few directions.

Discussion

The energy required for control is a significant issue for the practical control of complex systems. By exploring the eigen-space of the controlled system we found that the required energies along different directions of the state space are highly heterogeneous, indicating the existence of subspaces that are extremely difficult to control if only a subset of nodes are directly driven. Control can be energetically costly if we aim to control the system using only a few driver nodes, in which case the required energy increases exponentially with the system size. Our findings imply that complex systems, even those following linear dynamics, can not be steered towards certain final states via external control inputs. This may be the reason why, for example, transcriptional networks for gene expression⁴⁶ and sensorimotor systems for motion control⁴⁷ function only in a low-dimensional subspace.

Our work raises several questions for future work. First, *directed* networks have eigenvalues with imaginary parts, which can be addressed numerically using our framework (see SI Sec. V). We lack, however, analytical tools for general directed networks. Second, there are multiple configurations¹⁶ of driver (sensor) nodes that can yield the control (observation) of a network. We still lack efficient methods to choose the driver or sensor nodes that minimize the control energy or observation uncertainty for a given direction. Finally, linear dynamics (1) accurately captures the behavior of nonlinear systems in the vicinity of their equilibria, allowing us to reveal the fundamental control properties of networks⁴⁸. Nevertheless, further work is needed to cope with the impact of nonlinearity for large complex systems away from their equilibria.

1. Albert, R. & Barabási, A.-L. Statistical mechanics of complex networks. *Rev. Mod. Phys.* **74**, 47–97 (2002).
2. Cohen, R. & Havlin, S. *Complex Networks: Structure, Robustness and Function* (Cambridge University Press, 2010).
3. Newman, M. E. J. *Networks: An Introduction* (Oxford University Press, 2010).
4. Rugh, W. J. *Linear System Theory* (Prentice Hall, 1996).
5. Sontag, E. D. *Mathematical Control Theory: Deterministic Finite Dimensional Systems* (Springer, New York, 1998).
6. Slotine, J.-J. & Li, W. *Applied Nonlinear Control* (Prentice-Hall, 1991).
7. Liu, Y.-Y., Slotine, J.-J. & Barabási, A.-L. Controllability of complex networks. *Nature* **473**, 167–173 (2011).
8. Sorrentino, F., di Bernardo, M., Garofalo, F. & Chen, G. Controllability of complex networks via pinning. *Phys. Rev. E* **75**, 046103 (2007).
9. Yu, W., Chen, G. & Lü, J. On pinning synchronization of complex dynamical networks. *Automatica* **45**, 429–435 (2009).
10. Rajapakse, I., Groudine, M. & Mesbahi, M. Dynamics and control of state-dependent networks for probing genomic organization. *Proc. Natl. Acad. Sci. USA* **108**, 17257–17262 (2011).

11. Nepusz, T. & Vicsek, T. Controlling edge dynamics in complex networks. *Nat. Phys.* **8**, 568–573 (2012).
12. Yan, G., Ren, J., Lai, Y.-C., Lai, C.-H. & Li, B. Controlling complex networks: How much energy is needed? *Phys. Rev. Lett.* **108**, 218703 (2012).
13. Sun, J. & Motter, A. E. Controllability transition and nonlocality in network control. *Phys. Rev. Lett.* **110**, 208701 (2013).
14. Pasqualetti, F., Zampieri, S. & Bullo, F. Controllability metrics, limitations and algorithms for complex networks. *IEEE Trans. Control Netw. Syst.* **1**, 40–52 (2014).
15. Tang, Y., Gao, H., Zou, W. & Kurths, J. Identifying controlling nodes in neuronal networks in different scales. *PLoS ONE* **7**, e41375 (2012).
16. Jia, T. *et al.* Emergence of bimodality in controlling complex networks. *Nat. Commun.* **4**, 2002 (2013).
17. Yuan, Z., Zhao, C., Di, Z., Wang, W.-X. & Lai, Y.-C. Exact controllability of complex networks. *Nat. Commun.* **4**, 2447 (2013).
18. Ruths, J. & Ruths, D. Control profiles of complex networks. *Science* **343**, 1373–1376 (2014).
19. Menichetti, G., Dall’Asta, L. & Bianconi, G. Network controllability is determined by the density of low in-degree and out-degree nodes. *Phys. Rev. Lett.* **113**, 078701 (2014).
20. Menolascina, F. *et al.* *In-Vivo* real-time control of protein expression from endogenous and synthetic gene networks. *PLoS Comput. Biol.* **10**, e1003625 (2014).

21. Rahmani, A., Ji, M., Mesbahi, M. & Egerstedt, M. Controllability of multi-agent systems from a graph-theoretic perspective. *SIAM J. Control Optim.* **48**, 162–186 (2009).
22. Acemoglu, D., Ozdaglar, A. & ParandehGheibi, A. Spread of (mis)information in social networks. *Game Econ. Behav.* **70**, 194–227 (2010).
23. Liu, Y.-Y., Slotine, J.-J. & Barabasi, A.-L. Observability of complex systems. *Proc. Natl. Acad. Sci. USA* **110**, 2460–2465 (2013).
24. Yang, Y., Wang, J. & Motter, A. E. Network observability transitions. *Phys. Rev. Lett.* **109**, 258701 (2012).
25. Pinto, P. C., Thiran, P. & Vetterli, M. Locating the source of diffusion in large-scale networks. *Phys. Rev. Lett.* **109**, 068702 (2012).
26. Scheffer, M. *et al.* Anticipating critical transitions. *Science* **338**, 344–348 (2012).
27. Friedman, N. Inferring cellular networks using probabilistic graphical models. *Science* **303**, 799–805 (2004).
28. Almaas, E., Kovács, B., Vicsek, T., Oltvai, Z. N. & Barabási, A.-L. Global organization of metabolic fluxes in the bacterium escherichia coli. *Nature* **427**, 839–843 (2004).
29. Castellano, C., Fortunato, S. & Loreto, V. Statistical physics of social dynamics. *Rev. Mod. Phys.* **81**, 591–646 (2009).
30. May, R. M. *Stability and Complexity in Model Ecosystems* (Princeton University Press, 1974).

31. Pecora, L. M. & Carroll, T. L. Master stability functions for synchronized coupled systems. *Phys. Rev. Lett.* **80**, 2109–2112 (1998).
32. Chung, F., Lu, L. & Vu, V. Spectra of random graphs with given expected degrees. *Proc. Natl. Acad. Sci. USA* **100**, 6313–6318 (2003).
33. Kim, D. & Kahng, B. Spectral densities of scale-free networks. *Chaos* **17**, 026115 (2007).
34. Cohen, R., Erez, K., ben Avraham, D. & Havlin, S. Resilience of the internet to random breakdowns. *Phys. Rev. Lett.* **85**, 4626–4628 (2000).
35. Barabási, A.-L. & Albert, R. Emergence of scaling in random networks. *Science* **286**, 509 (1999).
36. Maslov, S. & Sneppen, K. Specificity and stability in topology of protein networks. *Science* **296**, 910–913 (2002).
37. Erdős, P. & Rényi, A. On the evolution of random graphs. *Publ. Math. Inst. Hung. Acad. Sci.* **5**, 17–60 (1960).
38. Watts, D. J. & Strogatz, S. H. Collective dynamics of ‘small-world’ networks. *Nature* **393**, 440–442 (1998).
39. Cowan, N. J., Chastain, E. J., Vilhena, D. A., Freudenberg, J. S. & Bergstrom, C. T. Nodal dynamics, not degree distributions, determine the structural controllability of complex networks. *PLoS ONE* **7**, e38398 (2012).
40. Everton, S. *Disrupting Dark Networks* (Cambridge University Press, 2012).

41. Kaiser-Bunbury, C. N., Muff, S., Memmott, J., Mller, C. B. & Caflisch, A. The robustness of pollination networks to the loss of species and interactions: a quantitative approach incorporating pollinator behaviour. *Ecology Letters* **13**, 442–452 (2010).
42. Newman, M. E. J. Assortative mixing in networks. *Phys. Rev. Lett.* **89**, 208701 (2002).
43. Girvan, M. & Newman, M. E. J. Community structure in social and biological networks. *Proc. Natl. Acad. Sci. USA* **99**, 7821–7826 (2002).
44. Bascompte, J., Jordano, P., Melin, C. J. & Olesen, J. M. The nested assembly of plant-animal mutualistic networks. *Proc. Natl. Acad. Sci. USA* **100**, 9383–9387 (2003).
45. Kailath, T., Sayed, A. & Hassibi, B. *Linear Estimation* (Prentice Hall, 2000).
46. Müller, F.-J. & Schuppert, A. Few inputs can reprogram biological networks. *Nature* **478**, E4 (2011).
47. Todorov, E. & Jordan, M. I. Optimal feedback control as a theory of motor coordination. *Nature Neurosci.* **5**, 1226–1235 (2002).
48. Whalen, A. J., Brennan, S. N., Sauer, T. D. & Schiff, S. J. Observability and controllability of neuronal network motifs. *arXiv* 1307.5478v2 (2013).

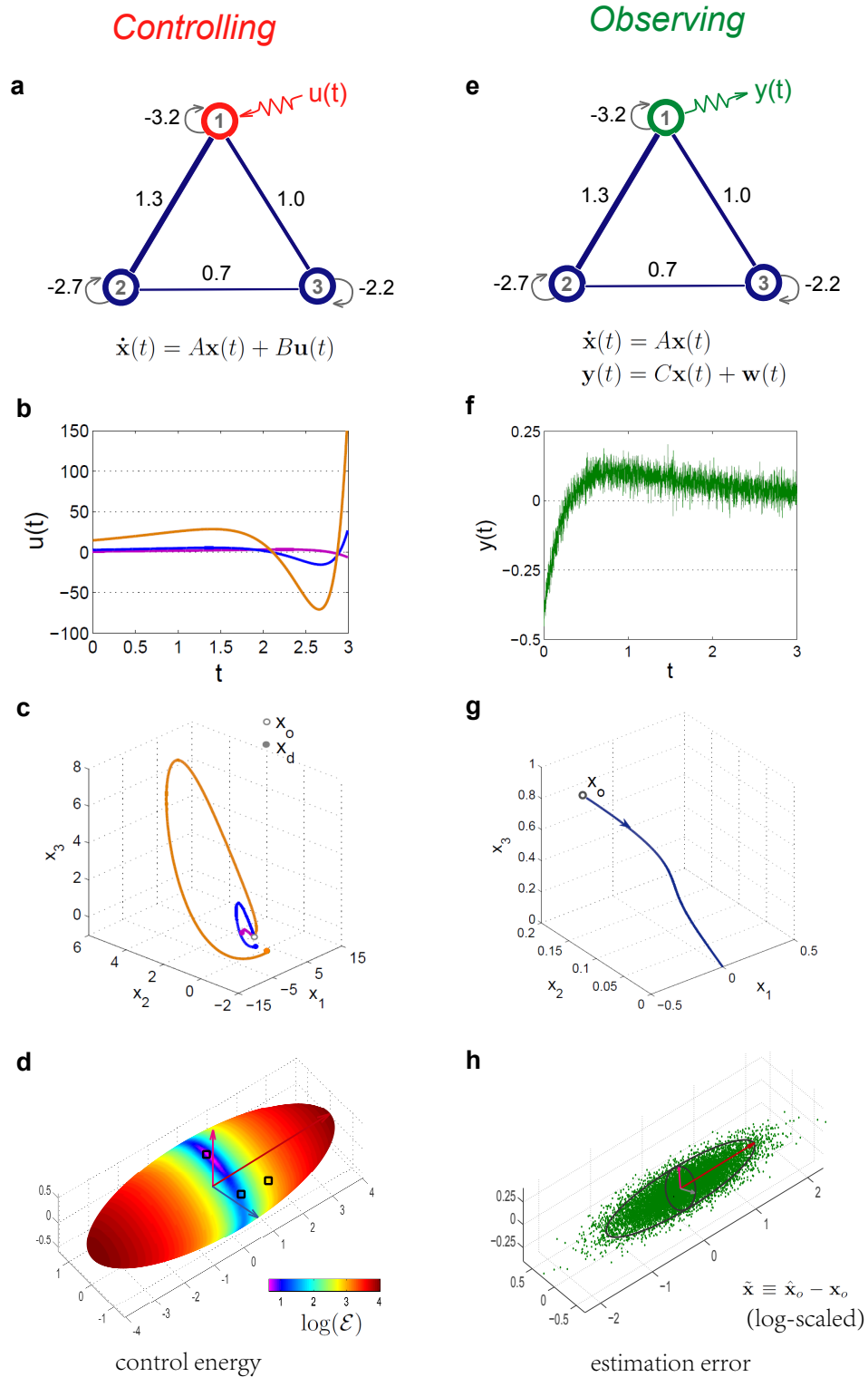


Figure 1

Figure 1: Controlling and observing a network. (a) Controlling a three-node weighted network with one external signal $u(t)$ that is injected to the driver node (red). Hence the input matrix $B = [1, 0, 0]^T$. The nodes have negative self-loops which make all eigenvalues of the adjacency matrix A negative. (b) Optimal control signals which minimize the energies required to move the network from the initial state $\mathbf{x}_o = [0, 0, 0]^T$ to three different desired states \mathbf{x}_d with $\|\mathbf{x}_d\| = 1$ in the given time interval $t \in [0, 3]$. (c) The trajectories of the network state $\mathbf{x}(t)$ driven respectively by the control signals in (b). (d) The energy surface for all normalized desired states, i.e., $\|\mathbf{x}_d\| = 1$, which is an ellipsoid spanned by the controllability Gramian's three eigen-directions (arrows). The squares correspond to the three cases depicted in (b) and (c). (e) Observing the network with one output $y(t)$. Node 1 is selected as the sensor (green) thus the output matrix $C = [1, 0, 0]$. $\mathbf{w}(t)$ is Gaussian white noise with zero mean and variance one. (f) A typical output $y(t)$ that will be used to approximate the initial state \mathbf{x}_o . (g) A typical trajectory of the system $\dot{\mathbf{x}} = A\mathbf{x}$ starting from $\mathbf{x}_o \neq 0$ towards the origin of the state space. (h) Estimation error $\tilde{\mathbf{x}} = \hat{\mathbf{x}}_o - \mathbf{x}_o$, where $\hat{\mathbf{x}}_o$ is the maximum-likelihood estimator. For one initial state we ran the system 5000 times independently, and each dot represents the estimation error of one run. The uncertainty ellipsoid (black) corresponds to the standard deviation of $\tilde{\mathbf{x}}$ in any direction.

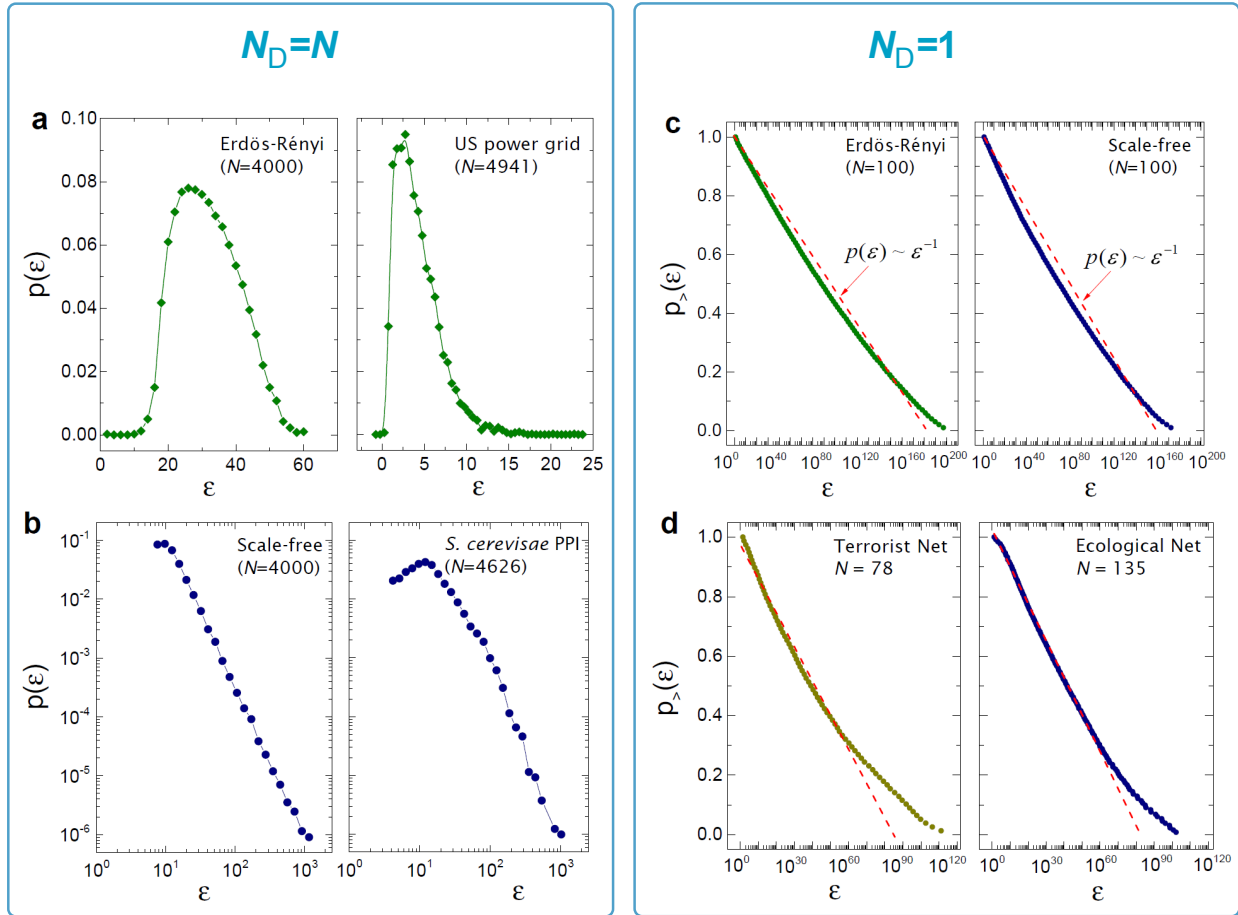


Figure 2

Figure 2: Control spectrum for complex networks. (a) The distribution of eigen-energies $p(\mathcal{E})$ for controlling an Erdős-Rényi model network³⁷ and the US power grid³⁸ with $N_D = N$ driver nodes, which are bounded. (b) The distribution of eigen-energies $p(\mathcal{E})$ for controlling a scale-free³⁵ and the *S. cerevisiae* protein-protein interaction³⁶ networks with $N_D = N$. (c) The complementary cumulative distributions $p_{>}(\mathcal{E})$ of eigen-energies for controlling an Erdős-Rényi and a scale-free network with $N_D = 1$. The dashed lines correspond to $p(\mathcal{E}) \sim \mathcal{E}^{-1}$. (d) The complementary cumulative distributions $p_{>}(\mathcal{E})$ of eigen-energies for controlling two empirical (terrorist communication⁴⁰ and mutualistic ecological⁴¹) networks with a single driver node ($N_D = 1$). The dashed lines indicate $p(\mathcal{E}) \sim \mathcal{E}^{-1}$. The edges' weights A_{ij} are drawn from $[0, 1]$ uniformly for all model networks. The self-loops $A_{ii} = -\sum_j A_{ij} - \delta$ where $\delta = 0.25$, a small perturbation to diagonal entries, to ensure that the network is stable.

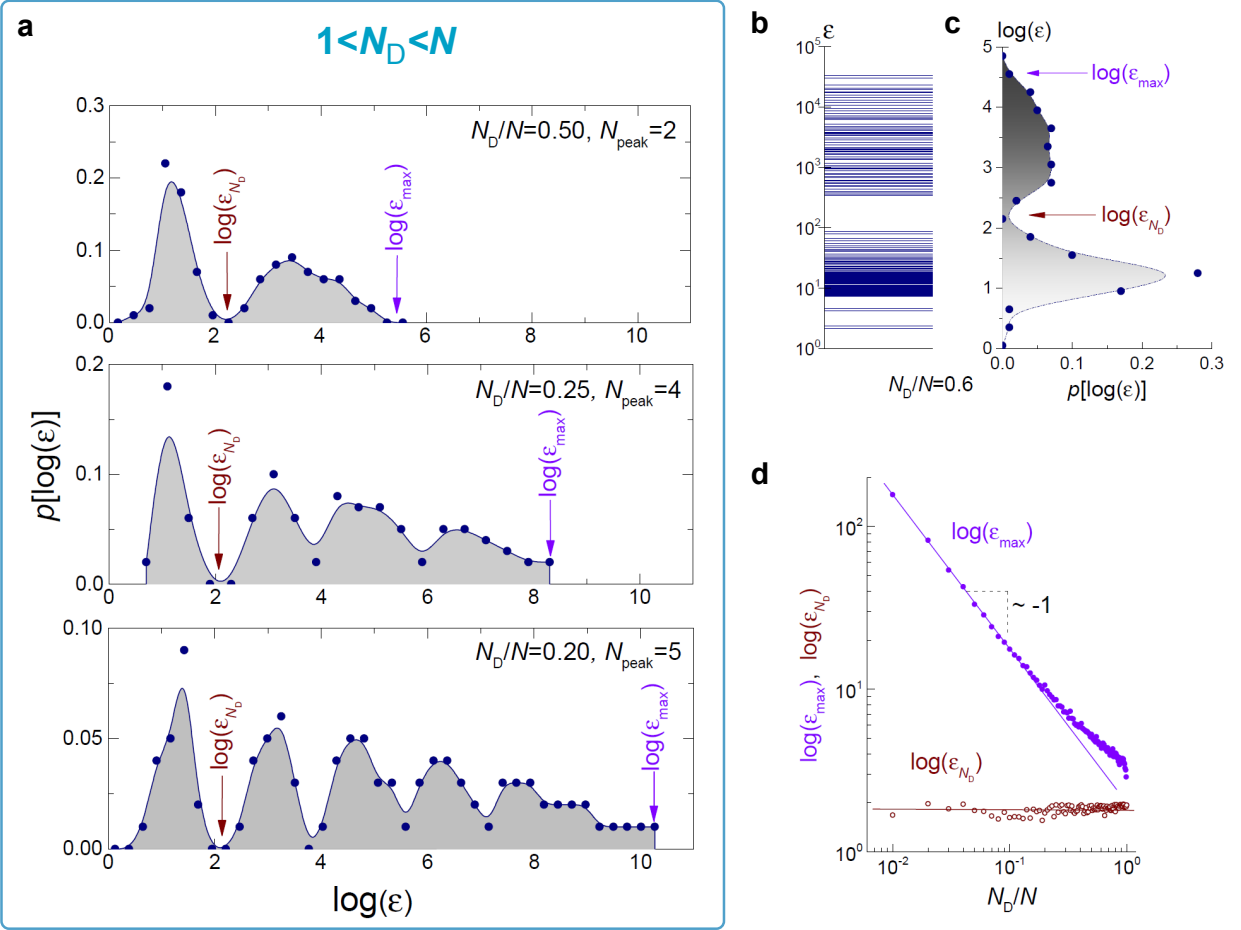


Figure 3

Figure 3: Control spectrum for driving a fraction of nodes. The network has $N = 100$ nodes, with degree distribution $p(k) \sim k^{-3.0}$ and average degree $\langle k \rangle = 10$. **(a)** The multi-peak distributions $p[\log(\mathcal{E})]$ for $1 < N_D < N$, where the dots represent numerical results. The solid curves and shaded areas are smoothed for illustration. \mathcal{E}_{N_D} denotes the boundary of the first energy band. \mathcal{E}_{\max} is the largest energy corresponding to the most difficult direction of the N -dimensional state space. We find that the number of peaks is given by $N_{\text{peak}} = \text{int}[N/N_D]$ (also see SI Fig. S3). **(b)** The eigen-energy spectrum for controlling the network. The fraction of driver nodes is $N_D/N = 0.6$. We observe a gap in the logarithmic scale between the N_D -th and the $(N_D + 1)$ -th smallest eigen-energies. This gap leads to the two-peak distribution of $p[\log(\mathcal{E})]$ in **(c)**. **(d)** $\log(\mathcal{E}_{N_D})$ and $\log(\mathcal{E}_{\max})$ as functions of N_D/N . We find that \mathcal{E}_{N_D} depends weakly on N_D , in contrast with $\log(\mathcal{E}_{\max}) \sim (N_D/N)^{-1}$, i.e., $\mathcal{E}_{\max} \sim e^{N/N_D}$.

Table 1: Controlling complex networks with different number of driver nodes

<i>Number of driver nodes</i>	<i>Distribution of eigen-energies</i>	<i>Largest energy</i>
$N_D = N$	$p(\mathcal{E}) \sim \mathcal{E}^{-\gamma}$	$\mathcal{E}_{\max} \sim N^{\frac{1}{\gamma-1}}$
$1 < N_D < N$	$N_{\text{peak}} = \text{int}[N/N_D]$ for $p[\log(\mathcal{E})]$	$\mathcal{E}_{\max} \sim e^{N/N_D}$
$N_D = 1$	$p(\mathcal{E}) \sim \mathcal{E}^{-1}$	$\mathcal{E}_{\max} \sim e^N$

N is the total number of nodes and N_D is the number of driver nodes. γ is the exponent of the degree distributions $p(k) \sim k^{-\gamma}$. When γ is large, the network becomes degree-homogeneous.